CO_2QUEST Newsletter

Summer 2016

CO_2QUEST

Impact of the Quality of CO_2 on Storage and Transport

Introduction

Welcome to the fourth edition of the EU FP7-funded-project CO_2QUEST newsletter, highlighting the most recent technical developments since the project's commencement in March 2013. The CO_2QUEST consortium, led by Prof. Haroun Mahgerefteh at University College London (UCL, UK) comprises 10 other partners: Bundesanstalt für Geowissenschaften und Rohstoffe (BGR, Germany), Uppsala University (UU, Sweden), Dalian University of Technology (DUT, PR China), Environmental & Water Resources Engineering Ltd. (EWRE, Israel), Imperial College London (ICL, London), Institut National de l'Environnement Industriel et des Risques (INERIS, France), National Centre for Scientific Research 'Demokritos' (NCSRD, Greece), Onderzoekscentrum voor Aanwending van Staal (OCAS, Belgium), CanmetENERGY (CANMET, Canada) and the University of Leeds (UoL, UK).

CO_2QUEST addresses the fundamentally important issues regarding the impact of the typical impurities in the gas or dense-phase CO_2 stream captured from fossil fuel power plants on its safe and economic transportation and storage. The above involves the determination of the important CO_2 mixtures that have the most profound impact on the pipeline pressure drop, compressor power requirements, pipeline propensity to ductile and brittle facture propagation, corrosion of the pipeline and wellbore materials, geochemical interactions within the wellbore and storage site, and the ensuing health and environmental hazards. Based upon a cost/benefit analysis and whole system approach, the results will in turn be used to provide recommendations for tolerance levels, mixing protocols and control measures for pipeline networks and storage infrastructure.

University College London, UK

Bundesanstalt fur Geowissenschaften und Rohstoffe, Germany

Uppsala Universitet, Sweden

Dalian University of Technology, China

Environmental & Water Resources Engineering Ltd., Israel

ICL, UK

Institut National de l'Environnement Industriel et des Risques, France

Demokritos, National Research Centre for Physical Sciences, Greece

Onderzoekscentrum voor Aanwending van Staal, Belgium

University of Leeds, UK

CanmetENERGY, Canada

This project has received funding from the European Union's Seventh Framework Programme for research, technological development and demonstration under grant agreement no 309102

CO_2QUEST Communication and Exploitation Event

H. Mahgerefteh and R. Porter

University College London, U.K.

The CO_2QUEST Communication and Exploitation Event was organised by Prof. Haroun Mahgerefteh and Dr. Richard Porter at University College London and was held on the College's Bloomsbury Campus on May 20th 2016. The purpose of the meeting was to present the major achievements of CO_2QUEST so to ensure that the project's advances are disseminated and fully exploited, enabling CCS technology to be deployed at an accelerated rate. The successful event was attended by 45 delegates of a diverse range of backgrounds that included representation from several industrial and legislative organisations as well as numerous academics. The agenda was split into two main areas, comprising firstly the recently constructed world class CCS experimental and pilot-scale testing facilities (then split into sub-categories for CO_2 pipeline transportation and CO_2 sequestration) and secondly CCS simulation software. This interesting agenda stimulated beneficial discussions both during the sessions and informally during breaks.

Figure 1. Prof. Haroun Mahgerefteh opened the event, providing an overview of the CO_2QUEST project and putting its major achievements into context.

Figure 2. Dr. Régis Farret presented an overview and the results obtained from the Senonian shallow aquifer CO_2 injection experimental testing facilities at INERIS, France.

Several presentations were made during the event and will be made available to download on the CO_2QUEST website. For further information please feel free to contact Richard Porter at UCL (r.t.j.porter@ucl.ac.uk).

Figure 3. Videos taken from the air by drone of CO_2 pipeline rupture tests were presented by Dr. Shaouyn Chen during his talk on the experimental CCS facilities in Dalian, China.

Geochemical Impact of Impure CO_2 on a Storage Reservoir – Spatial Development over Time

D. Rebscher[1], J.L. Wolf[1], J. Bensabat[2], and A. Niemi[3]

[1]Federal Institute for Geosciences and Natural Resources (BGR), Hannover, Germany
[2]Environmental and Water Resources Engineering Ltd. (EWRE), Haifa Israel
[3]Uppsala Universitet, Sweden

Within work package 3 of the CO_2QUEST project, impure CO_2 injection into a saline aquifer on a reservoir scale is simulated using the coupled thermal, hydrological, chemical code TOUGHREACT V3-OMP/ECO2N [Xu et al., 2014; Pruess 2005] from Lawrence Berkeley National Laboratory. The 2D radial model consists of four horizontal layers, i.e. from top to bottom caprock, sandstone, shale, and sandstone with respective heights of 2 m, 2 m, 3 m, and 9 m and a lateral extent of 30 km [Wolf et al., subm]. The initial pressure in the reservoir amounts to 14.7 MPa with a temperature of 66 °C. In the sandstones, horizontal and vertical permeabilities amount to 700 mD and 100 mD, respectively, whereas permeabilities in the shale and caprock were given isotropic values of 0.1 mD. Porosities range from 0.95 % in the shale and caprock, 15.6 % in the bottom sandstone to 21.3 % in the upper sandstone. The dominant primary minerals in the sandstone layers are mainly quartz, feldspars, clay minerals, and carbonates. Geological characteristics and injection parameters were chosen in accordance to the CCS pilot site Heletz in Israel as well as field and laboratory analysis performed in regard to this site [Niemi et al., in press].

A realistic injection scenario was chosen with a continuous injection rate of 9 kg/s including 1 mole % of SO_2 via an open well covering about three quarters of the lower part of the bottom sandstone layer. In order to identify as well as quantify the critical geochemical processes, alteration of the reservoir minerals and brine composition were simulated based on trace gas transport. Focusing on the reservoir rock, in general, three zones can be distinguished predominated by pressure, CO_2, and SO_2, respectively, spreading and moving away from the injection point as injection progresses in time, refer Figure 4. In the modelled time-span of ten years, the physical impact on the reservoir in terms of pressure changes of about 2 bar are simulated at a distance of more than 10 km to the injection well. Whereas the pressure footprint is large on the scale of the reservoir, the geochemically affected regions are smaller. Here, again, one has to distinguish between CO_2 and the impurity SO_2. As SO_2 dissolves preferentially into the brine, the co-injected CO_2 moves faster and farther within the sandstone, reaching a lateral extent of about 2000 m after ten years. The acidic impact of pure CO_2 leads to minor carbonate dissolution.

Dissolved SO_2 alters the mineral ankerite ($CaFe_{0.7}Mg_{0.3}(CO_3)_2$) of the Cretaceous reservoir rock into anhydrite ($CaSO_4$), resulting in a lateral extent of about 180 m after ten years. Given the mineralogy at Heletz, this results in a porosity increase of 0.5 percentage points of bulk volume. In the same time-span, a dry-out zone expands laterally about 70 m. Within this fully gas saturated zone emerging close to the injection well, further geochemical reactions are inhibited.

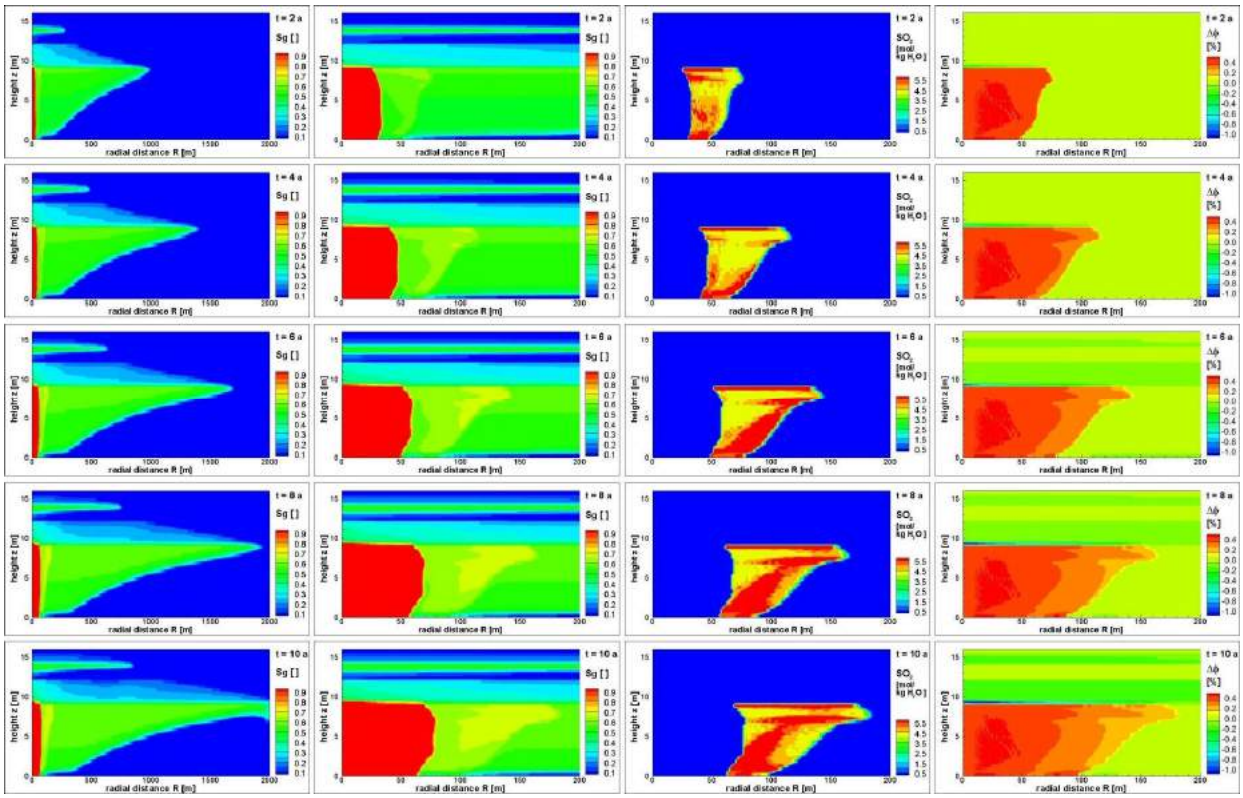

Figure 4. Development of three parameters in time and space: gas saturation Sg (column 1 and 2), sulfur dioxide in the aqueous phase $SO_2(aq)$, and porosity change $\Delta\phi$. First column to the left shows the development of the evolution of the CO_2 plume, reaching a lateral maximum of about 2000 m after ten years of injecting CO_2 with 1 % SO_2; zooming in around the injection well by a factor of 10, the emerging of a dry-out zone is distinctly visible as a red patch in these diagrams. Beyond this zone, where no further water rock interactions occur, lies the zone affected by $SO_2(aq)$, shown in the third column. Resulting porosity differences are presented in the forth column, at the very right. Note that all diagrams illustrate only the first 200 m of the 2D radial model, but column one, which depicts the first 2000 m of the total lateral extent of 30000 m.

Changes in the vertical direction are mainly based on the permeability and mineralogy of the geological layers, influenced by gravity effects, and the geometry of the injection well. At the border between the shale layer and the lower sandstone, a spatial separation of CO_2 and SO_2 occurs as CO_2 is able to penetrate into the shale, while SO_2 induces mineral alterations at first contact with the shale, resulting in a decrease of porosity of about 1 percentage points of bulk volume. Hence, this kind of “scrubbing effect” achieves a small additional sealing effect located directly above the lower sandstone reservoir.

Note that increase or decrease of porosity and their respective quantity depend on the initial mineral composition. Hence, the knowledge of the initial porosity distribution in a reservoir complex and understanding its changes due to the impact of flue gas injection might be of safety and economical interest as porosity influences permeability and the expense factors injectivity and storage capacity. In case of thick reservoir layers with high porosities, small changes might be negligible. However, in case of low porosity carbonate reservoirs and in rocks of high heterogeneity, porosity changes of a few percent might lead to significant shifts in the cost-benefit analysis. Therefore, a thorough selection of input parameter sets is required for qualitative reasonable predictions based on site-specific THC modelling.

References

A. Niemi, J. Bensabat, V. Shtivelman, K. Edlmann, P. Gouze, L. Luquot, F. Hingerl, S. M. Benson, P. A. Pezard, K. Rasmusson, T. Liang, F. Fagerlund, M. Gendler, I. Goldberg, A. Tatomir, T. Lange, M. Sauter, B. Freifeld, Heletz experimental site overview, characterization and data analysis for CO_2 injection and geological storage, *International Journal of Greenhouse Gas Control*, in press, 2016.

Pruess, K., ECO2N: A TOUGH2 fluid property module for mixtures of water, NaCl and CO_2, Report LBNL-57952, Lawrence Berkeley National Laboratory, Berkeley, CA, pp 76, 2005.

Wolf, J. L., Niemi, A., Bensabat, J., Rebscher, D., Benefits and restrictions of 2D reactive transport simulations of impurities co-injected with CO_2 in a saline aquifer, *International Journal of Greenhouse Gas Control*, subm.

Xu, T., Sonnenthal, E., Spycher, N., and Zheng, L., TOUGHREACT V3.0-OMP Reference Manual: A Parallel Simulation Program for Non-Isothermal Multiphase Geochemical Reactive Transport, Report LBNL-Draft, Lawrence Berkeley National Laboratory, Berkeley, CA, pp141, 2014.

Experimental Study of the CO_2 Pipeline Release from a Large-scale and a Buried Small-scale Pipeline

S. Chen, Y. Zhang, Y. Jianliang and X. Guo

School of Chemical Engineering, Dalian University of Technology, China

Objectives

- ✓ To conduct controlled large-scale experiments and buried small-scale experiments involving high pressure releases of CO_2 with a range of impurities, with near-field measurements of the dispersing jets, and temperature measurements in the vicinity of a pre-designed crack geometry.
- ✓ To validate the CFD model derived against experimental data available in the literature, and to be generated as part of the project as above.

Overview

In order to simulate a real CO_2 pipeline, a large-scale experimental pipeline with a total length of 258 m and the inner diameter of 233 mm and a buried small-scale experimental pipeline with a 25 mm inner diameter are developed to study the fluid dynamic behaviour of CO_2 pipeline blowdown. High frequency transducers were used to measure the evolution of fluid pressure after rupture. Thermocouples were installed to monitor the temperature distributions inside the pipeline. The pressure responses and phase transitions of different CO_2 phase were studied following pipeline rupture using different orifice diameters (Figure 5). In all the tests video recordings of the CO_2 dispersion cloud have been captured using a video camera setup on a radio controlled quadcopter (drone) (Figure 6).

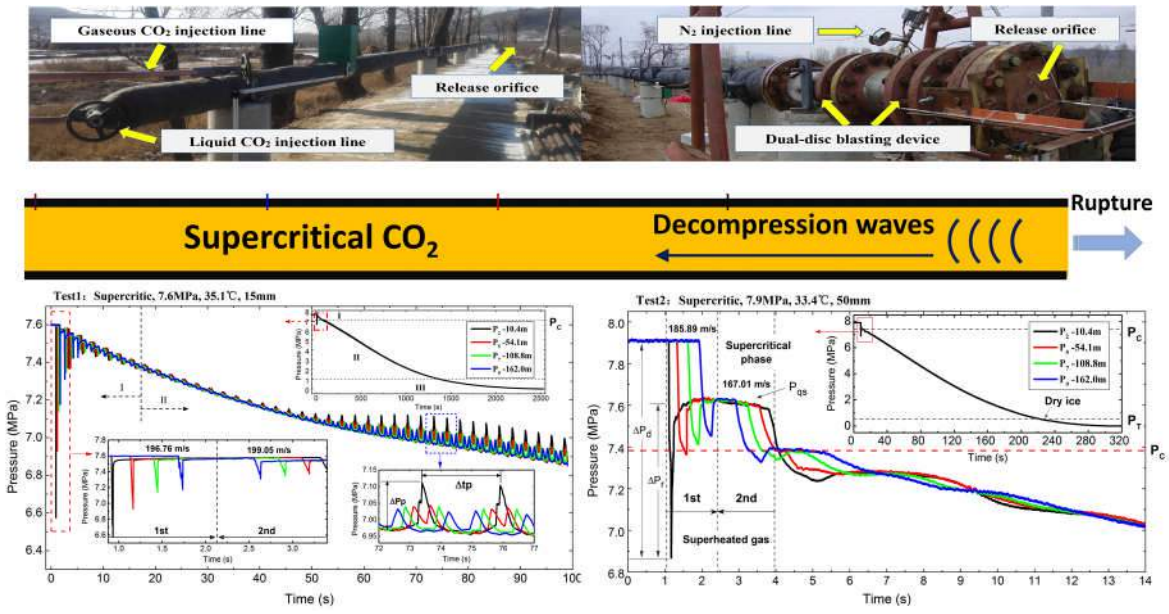

Figure 5. Large-scale CO_2 pipeline relief equipment and the pipeline pressure measurements taken in the decompression tests.

Figure 6. Visible cloud development of supercritical CO_2 release experiment with FBR.

In order to assess propensity of CO_2 pipelines to brittle fracture several experiments were performed using buried pipeline setup (Figure 7), though no crack propagation was observed in these tests. Nevertheless, it was found that the buried pipeline is rather dangerous than the exposed one. A large amount of CO_2 was trapped in the soil in the form of dry ice, which made the area full of high concentration CO_2 above the soil. The low temperature also may be a challenge for the buried pipeline which was under high pressure of CO_2.

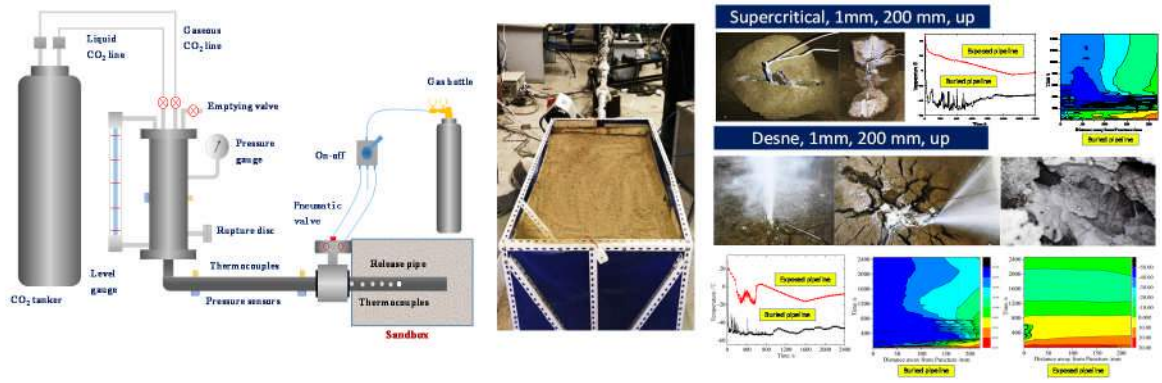

Figure 7. CO_2 release experiment using a buried small-scale pipeline.

Co-injection of CO_2 Key Impurities in a Single Well Push-Pull Experiment

R. Ronen and J. Bensabat

Environmental and Water Resources Engineering Ltd. (EWRE), Haifa Israel

Push-Pull is a field test aimed to study the geochemical and physical impacts of CO_2 with impurities in real geological conditions. In the Push-Pull experiment CO_2 with SO_2 and N_2 impurities is 'pushed' into the reservoir, and after few days the plume is 'pulled' back while monitoring and taking samples using the downhole sampling system. In this experiment we learn on the impacts of SO_2 on the reservoir brine and minerals, which will be most clearly observed as pH reduction. The N_2 injection has a physical impact of an increased pressure build-up due to the lower density of a CO_2-N_2 mixture. In this experiment we intend to consume 100 ton CO_2 with 2 wt% N_2 and 1 wt% SO_2.

CO_2 and SO_2 are hazardous and toxic chemicals; high concentration of them can be dangerous to humans. Therefore, safety procedure involves clear protocols, a list of emergency contacts and equipment to detect and deal with safety issues. On site there are three CO_2 detectors: (1) a carry on personal detector, (2) stationary detectors that are located in close proximity to the lines, and (3) laboratory detectors. The detectors in the laboratory allow monitoring the room carbon dioxide, methane, sulfur dioxide and oxygen concentrations. The site has fire safety equipment. Operators of the SO_2 system are required to wear a splash suit to protect them from getting exposed to sulfur dioxide. The SO_2 system design included a hazard analysis (HAZOP) that was supervised by an external expert. The N_2 design is completed as well. The components to the systems were purchased and the N_2 system is already assembled. Figure 8 shows the connection point of the SO_2 and N_2 systems to the CO_2 chemical injection line.

The downhole sampling system, a.k.a. U-tube, has three openings: drive, sampling and borehole inlet (Figure 9). Brine from the well enters the tube and reaches a depth of 200 meters below the ground level, which is the hydrostatic head condition. To extract the brine sample, we insert compressed nitrogen at 220 bar through the drive opening, which causes the check valve at the borehole inlet to close. This pressure drives the sample outside of the tube into the control panel. Then the nitrogen is removed by opening both ends of the U-tube to the atmosphere. This allows a new sample to enter the tube. The part of the

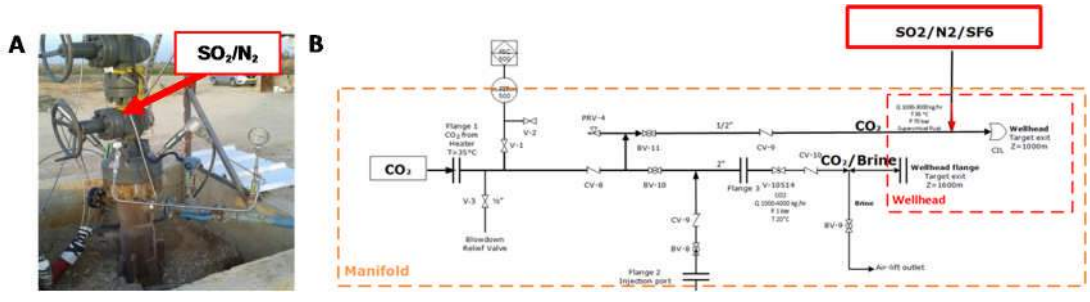

Figure 8. (A) photo of the SO_2 and N_2 systems' connection point to the chemical injection line on the wellhead. (B) Graphical system design that shows the connection point of the impurities lines to the CO_2 line.

sample that was exposed to air and nitrogen is thrown away, as this exposure can change the gas composition. In the onsite laboratory we are able to measure the sample in low and high pressure. Low pressure measurements include pH and conductivity, gas composition using quadrupole mass spectrometer and alkalinity. High pressure measurements include scaling of a cylinder full with a pressurized sample to indicate the sample's density, conductivity and pH, temperature and gas partial pressure.

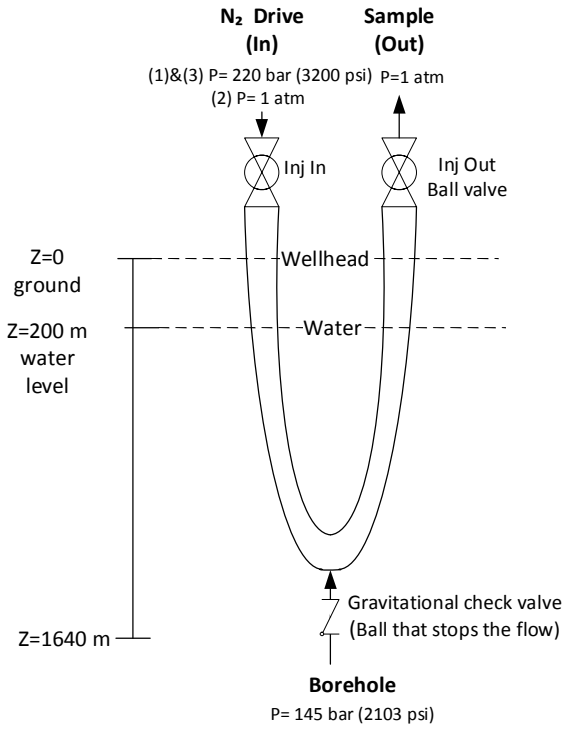

Figure 9. Simplified structure of the downhole sampling system - U-tube. The brine in the U-tube reaches 200 m below ground level, due to hydrostatic head condition. A check valve at the borehole inlet allows brine to enter the system when the pressure in the U-tube is below the reservoir pressure, and it limits the flow from the U-tube to the reservoir.

While operating the U-tube system we tested the system for leaks, our observation was that the U-tube system did not hold pressure, while the pressure in the casing, surrounding the u-tube increased. Eventually, we were unable to uplift a sample from within the injection well. In our system the U-tube has a concentric configuration – known as tube in tube configuration. The drive is the inner tube. Therefore, we concluded that there is a leak in the outer tube. To find the exact location of the leaks, we separated the problem to two areas: above ground and underground. If the leaks were on the surface it would have been easy to fix, so we tested the connections and pumped dye solution in search of leaks, but no leaks were found above ground. To test for underground leaks we used the distributed temperature sensing system DTS. DTS measures the temperature every 1 m with accuracy of ±0.06°C. We compared the temperature when injecting N_2 to the temperature of a tube filled with air (Figure 10). N_2 gas leaks through cracks, expands and lowers the temperature in the area according to Joule–Thomson effect. In the injection well four leak points were found, and we are unable to uplift samples. In the monitoring well two leak points were found, and the samples uplifting system is still able to operate, but large amount of N_2 gas are consumed. To conclude, both injection and monitoring well has leak points in their U-tube system. These cracks propagated over time. The cracks occurred due to mechanical failure or chemical failure (i.e., corrosion). "Sagerider" Company, which installed the U-tube, is working on adding new and improved tubes. To avoid failure, these new tubes will be made of Inconel superalloy (Alloy 600) that is rich of nickel-chromium and tested at 3800 psi.

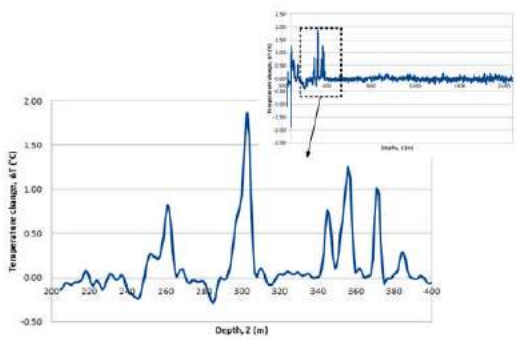

Figure 10. Leak test of the U-tube downhole sampling system. The temperature change along the well was measured using a distributed temperature sensing system (DTS). The y-axis shows the change in temperature when a system filled with air is injected with N_2 that leaks through the cracks.

To prepare the onsite laboratory, the gas composition measurement device "Quadrupole Mass Spectrometer (QMS)" was calibrated. QMS is used to study the mass-to-charge (m/z) ratio and abundance of gas phase ions. The abundance is given as ion current. To find the concentration of components in an unknown sample one needs to link between a known concentration and ion current. To calibrate the device for CO_2, three different and known concentrations of CO_2 were measured. We repeated the measurements twice and observed only small deviation. For example, calibration of CO_2 involved filling a sampling bag with 99.9% CO_2 diluted with N_2. The bag was connected to the QMS device, which produced readings of ion current versus atomic mass. The ion current of the highest peak CO_2, with largest abundance, that belongs to CO_2 at 44 amu was normalized and used to produce the graph in Figure 11.To conclude, the calibration equation will allow us to know the real CO_2 concentration based on the measured ion current. The QMS will also be used to measure the CO_2 percentage change over time, which indicates the plume spreading.

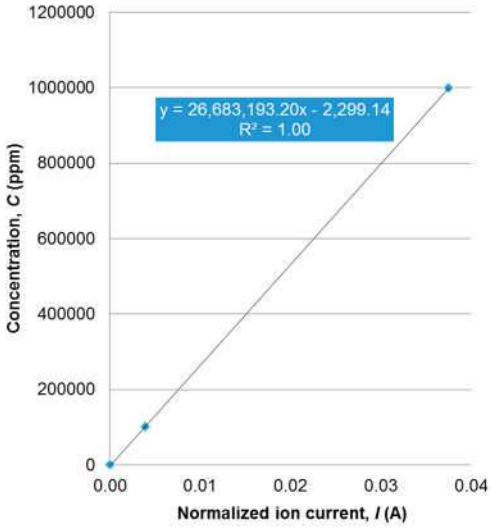

Figure 11. CO_2 gas calibration curve that links between normalized ion current and concentration.

Effects of Combined Interactions of Impurities on Operational Safety

S. Masoudi-Soltani, N. Mac Dowell and N. Shah

Imperial College London, UK

In this study, the interaction effects among several impurities including water, oxygen, NO_2, SO_2, Cl and several heavy metals (i.e. Pb, Hg, Cd and As) in the captured CO_2 stream on several safety criteria (i.e. corrosion, acute toxicity and chronic toxicity) have been investigated in order to define the resulting safe and unsafe operational envelopes during CO_2 transportation and storage phases.

Having the safety indices for individual impurities and their corresponding safety criteria at hand, the interactions among several impurities on one safety criteria were revealed by initially developing a full factorial DoE framework and then implementing an additive approach to represent the combined indices in each run. These interaction were next amalgamated in order to produce the corresponding 3D and contour plots which highlight the boundaries between the safe and unsafe operating conditions.

The combinations of impurities used in the development of the DoE tables are shown in Table 1.

As for a representative example, the 3D surface and contour plots for the corrosion are depicted in Figure 12 and 13, respectively.

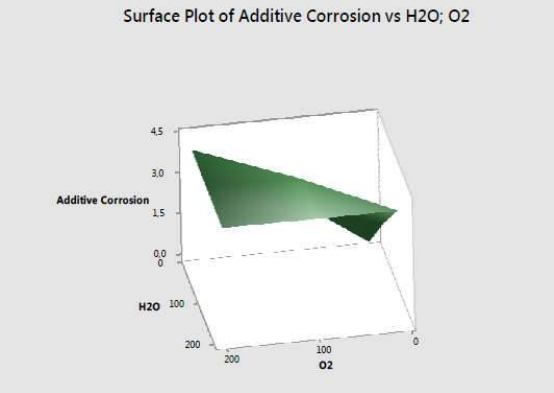

Figure 12. 3D surface plot representing the interaction effects between H2O and O2 on corrosion.

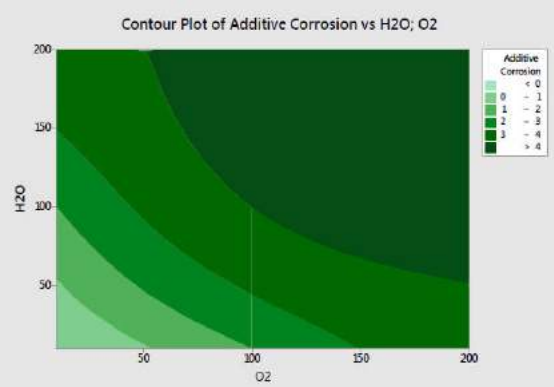

Figure 13. Contour plot representing the interaction effects between H_2O and O_2 on corrosion.

Factor	Effect	No. of Levels for Each Factor	No. of DoE Runs
O_2 & H_2O	Corrosion	3	$3^2 = 9$
SO_2, NO_2, Cl	Acute Toxicity	5	$5^3 = 125$
Pb, Hg, Cd, As	Chronic Toxicity	5	$5^4 = 625$

Table 1. Impurities (Factors) and their corresponding safety criteria (Effects) used in full factorial DoE development.

The Effects of Impurities along the CCS Chain

R. Farret, A. Ceroni and Y. Flauw

Institut National de l'Environment Industriel et des Risques, France

To fulfil the objectives of CO_2QUEST global assessment, INERIS proposed a tool to estimate the different effects (or impacts) of various impurities of a CO_2 stream all along the CCS chain. After a review of risk analyses for CCS -performed by INERIS or by other authors[1]- completed by the expertise of CO_2QUEST partners, we identified all relevant effects for impurities and we divided them in three categories. Then, the 5 most relevant "indicators" were selected to represent all these effects.

i) Physical effects. They are consequences such as reduced storage capacity or increased energy cost (for injection), but they do not prevent the "normal" evolution of the CCS project, contrary to the two following categories, that refer to CO_2 leakages. Finally, the only indicator that was finally retrained is CO_2 stream density, since it is the major factor for all physical effects identified.

ii) Chemical effects. They may increase the probability of leakage. The two main factors are pipe corrosion and degradation of well cement, hence the 2 selected indicators were Corrosivity (for pipes) and Acidity of the stream.

iii) Toxical/ecotoxical effects. They may increase the consequence if a leakage occurs - e.g., by contaminating an aquifer).
Acute toxicity of impurities and Ecotoxicity (possibly causing long-term effects) were selected as indicators.

In order to perform a global assessment, we chose a semi-quantitative approach, that is very common in risk analysis, and that is especially recommended when there is a need to compare a large range of phenomena, such as here. For each selected indicator, we proposed a scoring scale ranging from 0 to 4. For each impurity, score 4 on each indicator is

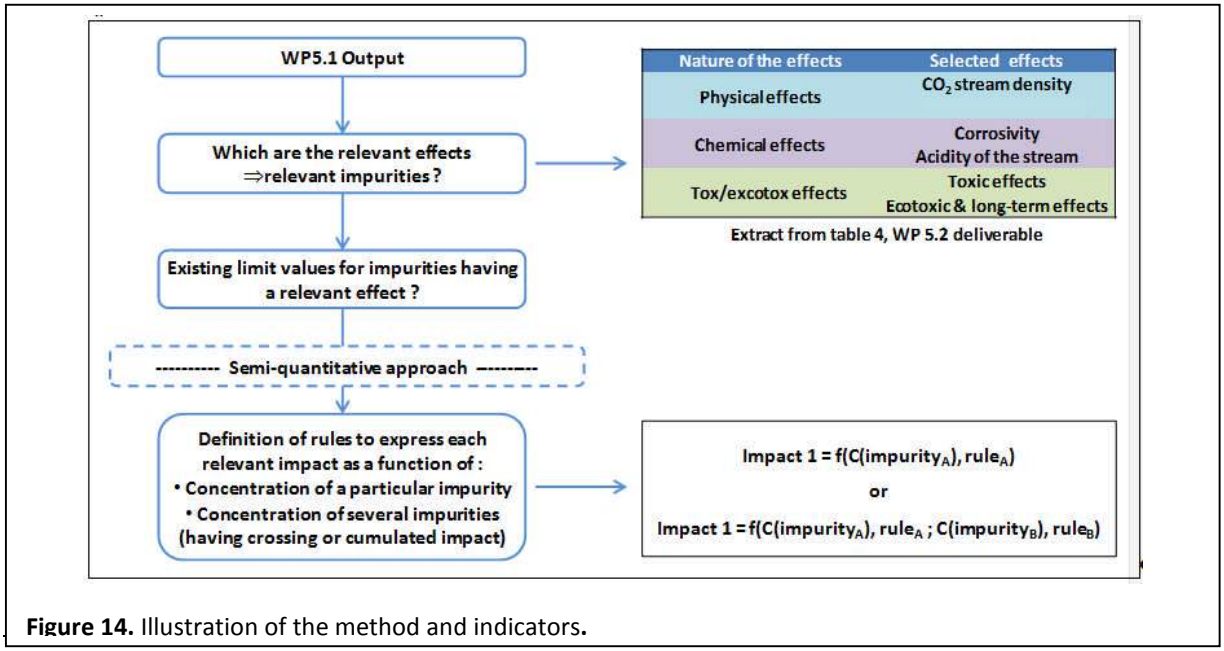

Figure 14. Illustration of the method and indicators.

[1] Mainly Farret et al., 2011ª, 2011b; Birkholtzer et al., 2009; Condor et al., 2010; Oldenburg, 2006; Savage et al., 2004; Dodds et al., 2011, Wilday et al., 2011. Numerous other publications were also considered, either related to methodologies for risk assessment or for the description of mechanisms and their modelling.

associated to a non-acceptable level (or non-acceptable effect), given by threshold values from regulation or from literature.

For each indicator, additive rules are defined to deduce the score for a whole CO_2, from the results for individual impurities. The 5 individual indicators are then displayed. The scores of these 5 indicators can also be summed up in order to give a global "impact index", that can in turn be combined with other social or economic criteria, e.g. in a cost-benefit analysis such as in WP4. A secondary global index is the number of "flags" that account for individual impurities that meet the threshold (maximum acceptable contents i.e., score 4).

A dedicated software tool was developed, based on a spreadsheet that displays all relevant impurities and all their possible effects and related thresholds. This assessment tool was applied to a series of CO_2 streams that were identified for 4 different capture processes. Typical CO_2 stream used as examples have been established on the basis of WP1.1 output, completed with data from other publications from INERIS and French CO_2-Club.

For each of these 4 capture processes, we considered two options:
1°) an optimum purification (low impurity contents), that is a "normal case".
2°) a "worst case" (with a maximum impurity contents). This case allows a better comparison between the technologies and brings information about the effects that are to be feared in case of a malfunction in the capture/purification process.

The results are displayed in Table 2.

Capture Process	Score (&flags) for "pure" CO_2 streams	Score (& flags) for "worst case" CO_2 streams
Oxyfuel combustion w. double flash	**5** (1)	**14** (2)
Oxyfuel combustion w. distillation	**6** (0)	**9** (2)
Post-combustion	**6** (1)	**9** (1)
Pre-combustion	**6** (0)	**14** (3)

Table 2. Results from the dedicated assessment tool for four capture processes.

An important result is that with "normal cases", all processes get a similar global note, that is rather low (5 or 6) with a limited number of "flags" (maximum 1) – see Table 2 – even if there are differences among the individual indicators – see Figure 15. Only when we consider "worst cases", a meaningful difference appears, showing that post-combustion and oxyfuel with distillation are likely to be less problematic.

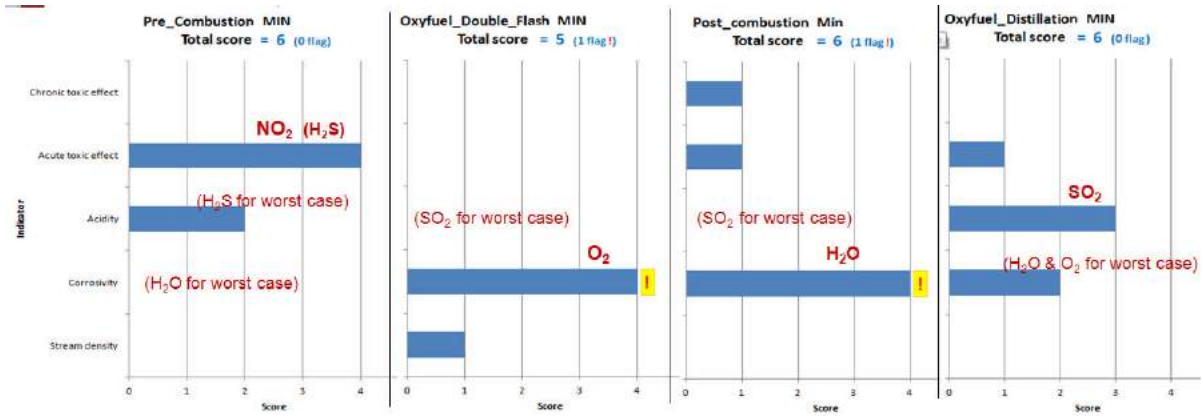

Figure 15. Global scores and number of flags for the 4 capture processes, for normal cases. Detail of the 5 indicators (blue bars) and identification of the most impacting impurities (red).

It is also interesting to compare the 5 different indicators:

- Corrosivity appears to be the most problematic indicator. It concerns most of the studied streams, and often with very high score (4/4). That may be due to the quite demanding (conservative) thresholds settled for both H_20 and O_2 impurities. Nevertheless pre-combustion stream shows that a low score is still possible to reach.
- Stream density and chronic ecotoxicity appear not to be major issues (the scores do not exceed 2, even with "worst cases"). However, for Chronic ecotoxicity, such a conclusion must be put into perspective because:
    - real impacts of a very long term pollution is not well known, and one may consider the simple presence of these impurities in a geological layer as an issue ;
    - Into the CO_2 streams studied in our example, information about MEA concentration was missing. This data could have a great impact, given the possibility that amines are degraded into nitrosamines that are well-known, very toxic components for water

Finally, we can easily identify that 5 substances explain most of the high notes for all criteria and all capture processes: SO_2, O_2, NO_2, H_2O, H_2S. Hence, for future studies, they should be the priority substances in terms of risks and potential impacts. H2, N2 and Hg can also to be considered in second priority.

References

Birkholzer, J.T., Zhou, Q., Tsang, C.F., 2009. Large-scale impact of CO_2 storage in deep saline aquifers: a sensitivity study on the pressure response in stratified systems. International Journal of Greenhouse Gas Control, Vol.3, Issue 2, 181-194.

Condor, J., Unatrakarn, D., Wilson, M. Asghari, K., 2011. A Comparative Analysis of Risk Assessment Methodologies for the Geologic Storage of Carbon Dioxide. Energy Procedia 4, 4036-4043.

Dodds, K., Watson M., Wright I., 2011. Evaluation of Risk Assessment Methodologies Using the In Salah CO_2 Storage Project as a Case History. Energy Procedia 4, 4162-4169.

Farret R., Manceau J-C., Le Gallo Y., Neuville N., 2011a. Note de synthèse Tâche 2.2: Identification de scénarios de risques de référence pour un complexe de stockage de CO_2, Convention n° 1094C0003 Ademe-GEOGREEN.

Farret R., André L., Brosse E., Broutin P., Chopin F., Gombert P., Jallais S., Saysset S. (2012) "Substances Annexes au CO_2 pour un Stockage Souterrain (SACSS) - Rapport du Groupe de Travail du Club CO_2, réf. INERIS-DRS-12-127545-07346A Farret et al, SACCS (2012).

M. Mohitpour, P. Seevam, K.K. Botros, B. Rothwell, C. Ennis, Pipeline transportation of carbon dioxide containing impurities, ASME Press, New York, NY, USA (2011).

Oldenburg, C.M., 2008. Screening and Ranking Framework for geologic CO_2 storage site selection on the basis of health, safety and environmental risk. Environmental Geology54, 1687-1694.

Savage, D., Maul, P.R., Benbow, S., Walke, R.C., 2004. A generic FEP database for the assessment of long-term performance and safety of the geological storage of CO_2. Quintessa Report QRS-1060A-1.

Wilday J., Paltrinieri N., Farret R., Hebrard J., Breedveld L., 2011. Addressing emerging risks using carbon capture and storage as an example, Process Safety and Environmental Protection 89, 463-471.

Development of Near-Field Dispersion Model

M. Fairweather, S.A.E.G. Falle, S. Van Loo, C.J. Wareing and A.M.E. Ward

University of Leeds, UK

Work is nearing completion regarding the development of a three-dimensional CFD model capable of predicting the near-field structure of high pressure releases of CO_2 containing impurities. At this stage, an impurity level of 4% N_2, typical of that to be expected in an integrated CCS chain, is being considered. The TREND impure equation of state [1] was found to have the capability needed for implementation within the CFD model and was selected for the work reported here. The complete model has been validated against experimental data available in the literature and against data generated as part of this project, for both pure and impure releases of CO_2. From the literature, data from the CO_2PIPETRANS, COOLTRANS and CO_2PIPEHAZ projects has been used, as well as experimental data from the UK Health and Safety Laboratory [2]. Examples of this validation are shown in Figure 16 pure CO_2 releases, and in Figure 17 for both pure and impure CO_2 releases.

Figure 16 compares centreline temperature predictions with varying liquid fraction at the release point to centreline experimental temperature data. The experimental data are seen to be coincident, within experimental error, up to 100D, after which the various experimental datasets diverge, with temperatures approaching ambient at different rates. Beyond 100D, the 100% liquid fraction prediction remains the coldest of the three predictions into the far-field, bracketing the coldest extremes of the data. The warmest extremes of the data are HSL Tests C and D, and these are captured by the 60% liquid prediction. The 80% liquid prediction falls half-way between the 60% and 100% predictions, indicating that DS1 Test 11 may have had a liquid fraction at the nozzle of

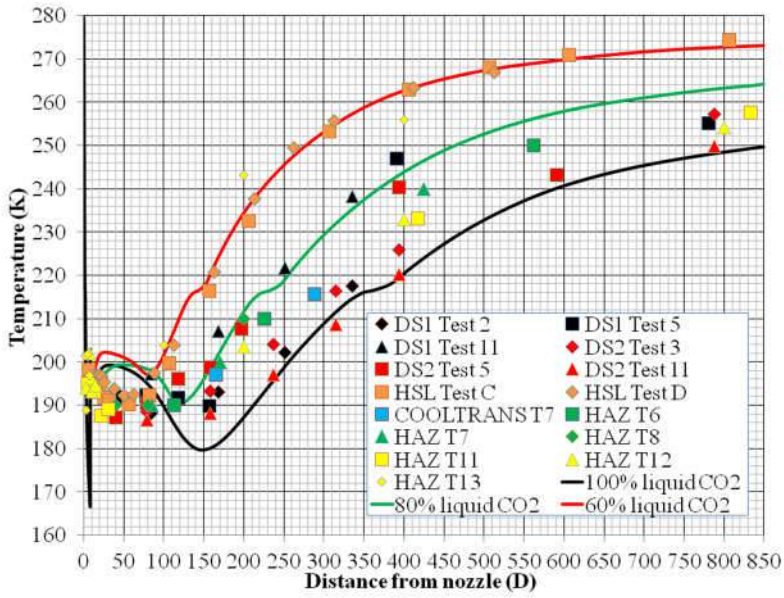

Figure 16. Experimental data (points) versus predictions (lines) of temperature along the centreline of an expanding liquid CO_2 jet release. Multiple datasets are identified in the legend and every data point should be assumed to have a 5°C error, not shown in the figure. Predictions are shown based on the COOLTRANS T7 inlet conditions for 60%, 80% and 100% liquid fraction at the nozzle.

around 80%. The variation in experimental data, though all were releases from high pressure (close to) 100% liquid reservoirs, can be explained by variation of the liquid fraction at the release point, as differences in the experimental rigs used ranged from direct release from a reservoir, to releases from elongated narrow-diameter pipes. Radial comparisons with data, not shown, at 80D, 100D, 165D and 400D along the centreline of the jets were also found to bracket the lower temperature extremes of the data, with good agreement found between the multiple datasets and predictions across the entire range of centreline locations.

Figure 17 shows a near-field comparison for both pure and impure CO_2 releases. Near-field data and predictions up to 40D from the release point are shown for both cases. In the pure CO_2 case, the data are generally consistent, with the numerical model able to predict these data. Within the Mach shock structure ($z < 8$ D), experiment and prediction do not agree well, although the data show some indication of an upward trending temperature close to the release point. Given the rapid variation of pressure just before the Mach shock, the rapid expansion and decrease in density, and the large acceleration to the shock, it is unlikely that the thermocouples used experimentally were able to capture the near-field detail. Beyond the Mach shock, however, prediction and measurement come in line.

For impure CO_2, multiple impure experimental datasets and two predictions are shown. The datasets are consistent, and reasonably well predicted. Interestingly, the recorded dispersion temperatures are very similar to those in the pure CO_2 experiments and show no clear difference between the type of impurity or the amount of impurity. This is supported by the close similarity of pure and impure predictions. Overall, these results further validate the numerical approach for the prediction of such releases, and highlight the significance of the mixture fraction at the release point, over the mixture composition itself.

Work regarding the representation of solid heat conduction in the CFD model, providing the capability of modelling heat transfer across a pipe wall which is of use to crack propagation predictions, is also nearing completion. The implementation of heat conduction was tested by comparing analytic and numerical results for the equilibrium

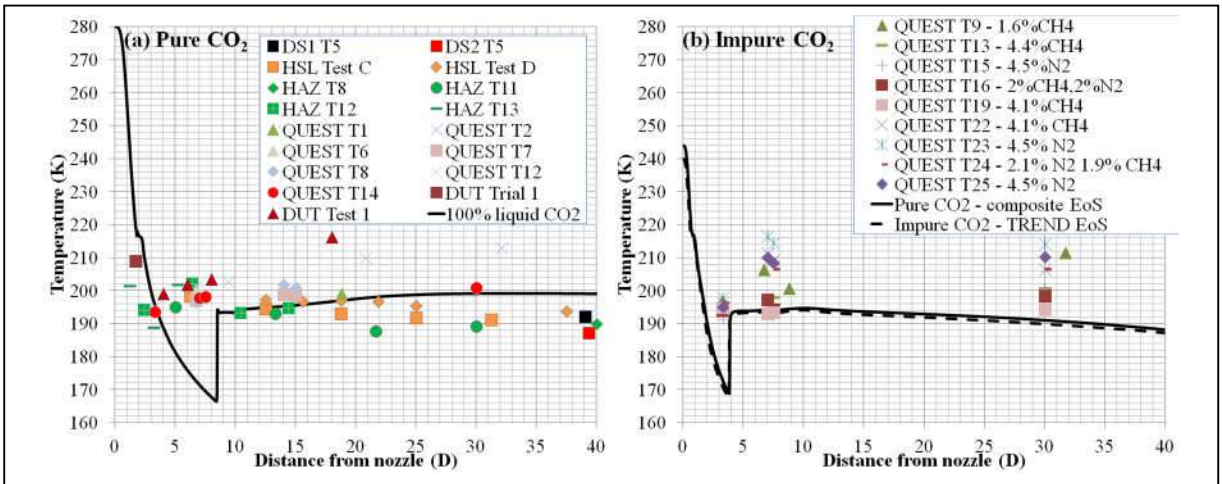

Figure 17. Experimental centreline near-field temperature data (points) for (a) pure and (b) impure releases of CO_2 from a high pressure reservoir. Multiple datasets are identified in the legends and every data point should be assumed to have a 5°C error, not shown in the figures. Shown also are predictions of the temperature (lines) based on the COOLTRANS T7 inlet conditions for 100% liquid fraction in (a) and based on pure and impure CO_2 inlet conditions in (b), matching reservoir conditions in CO2QUEST INERIS T12 (QUEST T12 in the diagram).

temperature distribution in a solid slab. Then, the numerical code was used to model high pressure releases of CO_2 and to obtain temperature results in the vicinity of a pre-designed crack geometry. The set-up of the simulation was similar to INERIS experiment 26 carried out as part of the project. Outflow conditions at the orifice were provided by UCL. The model was run until dynamic equilibrium was attained. The flow conditions were then fixed in the computational domain to further calculate the heat transfer within the pipe. Such an approach is necessary as the time scale for thermal equilibrium in the pipe is two orders of magnitude longer than for dynamic equilibrium in the CO_2-air mixture and would be otherwise computationally prohibitive. Fig. 18 shows the temperature distribution with time for one of the releases. The predictive approach adopted neglects heat transfer between the pipe and the gas and the obtained temperatures are seen to be marginally higher than in the experiments, but agree within the experimental measurement errors. Further work to improve these predictions is underway, and recent work that accounts for boundary layer cooling has been shown to produce predictions in line with the lower temperatures measured in Fig 18. Hence the two sets of predictions are able to bracket the temperature extremes noted in the experiments. Note that in the latter figure, the temperatures indicated by thermocouple T1 are not representative since this thermocouple became dislodged during the course of the experiment. Work to improve these predictions, and to compare them against further data sets, continues.

References

[1] Span, R., Eckermann, T., Herrig, S., Hielscher, S., Jager, A., Thol, M., 2015. TREND. Thermodynamic Reference and Engineering Data 2.0.1 Lehrstuhl fuer Thermodynamik, Ruhr-Universitaet Bochum.

[2] Pursell, M. 2012, Experimental investigation of high pressure liquid CO_2 release behaviour. In: IChemE Symposium Series No. 158, IChemE, pp. 164-171.

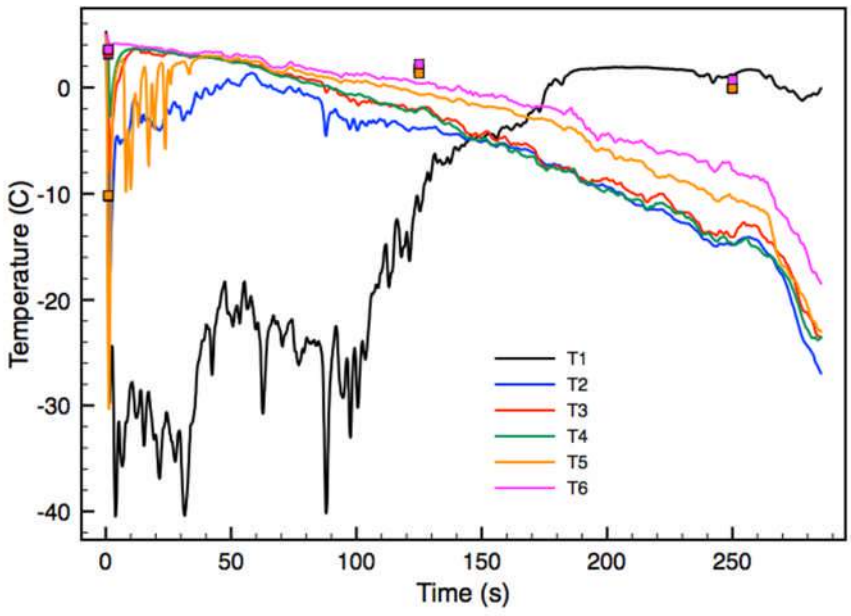

Figure 18. Comparison of numerically obtained temperatures (symbols) at the different thermocouples with data from INERIS for experiment 26 (lines).

Development of a Thermodynamic Model for CO_2 Solubility in Electrolyte Solutions and Brines Using Statistical Associating Fluid Thoery

I.G. Economou,[1,*] H. Jiang,[2] and A.Z. Panagiotopoulos[2]

[1]National Center for Scientific Research "Demokritos", Institute of Nanoscience and Nanotechnology, Molecular Thermodynamics and Modelling of Materials Laboratory, Aghia Paraskevi, Greece
[2]Department of Chemical and Biological Engineering, Princeton University, USA

Modeling of CO_2 solubilities in electrolyte solutions and especially in formation brines is of great improtance to the design of a CO_2 geological sequestration process. Most of the models in literature, which generally require many fitting parameters, focus on the CO_2 solubility in single NaCl solution. At the same time, CO_2 solubility in mixed electrolyte solutions and brines has not been studied by advanced equation of state. In this work, a thermodynamic model based on the statistical associating fluid theory (SAFT) was developed to study CO_2 solubilities in single and mixed electrolyte solutions, as well as synthetic formation brines. The proposed SAFT2-KMSA model implements an improved mean spherical approximation in the primitive model to handle the ion-ion electrostatic interactions, using a parameter *K* to correct the excess energies ("KMSA" for short). With the KMSA, the proposed model correlates accurately the activity coefficients and liquid densities of electrolyte solutions including Na^+, K^+, Ca^{2+}, Mg^{2+}, Cl^-, Br^-, and SO_4^{2-} over a wide range of temperature with only temperature-dependent parameters for the volume of anions. A representative example is shown in Figure 19, for the activity coefficient of NaCl in H_2O at different temperatures and compositions.

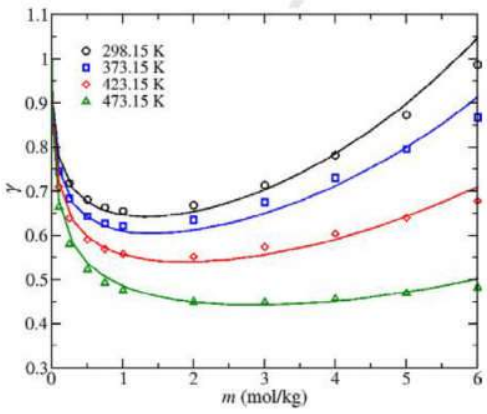

Figure 19. Activity coefficient of aqueous NaCl solution from 298.5 to 473.15 K. Symbols are literature experimental data and lines are SAFT2-KMSA calculations.

CO_2 is modeled as a nonassociating molecule and its solubilities in H_2O and single-electrolyte solutions are calculated using temperature-dependent CO_2 – H_2O and CO_2 – Ion binary interaction parameters. In Figure 20, the CO_2 solubility in aqueous NaCl solutions at various temperatures is shown. The model captures accurately the so-called salting-out effect.

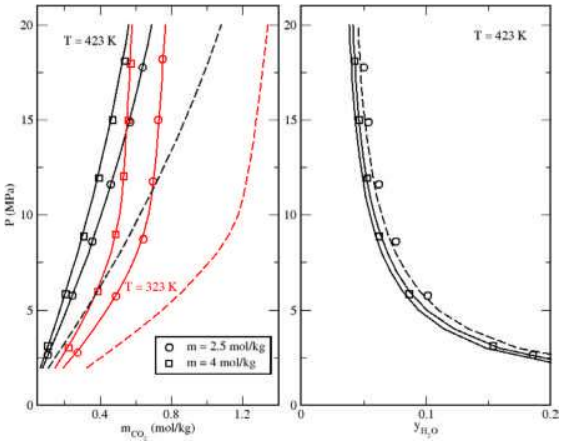

Figure 20. CO_2 solubility in aqueous NaCl solutions in terms of molality (left) and mole fraction of H_2O in the vapor phase (right) at 323 K and 423 K. Symbols are literature experimental data, solid lines are SAFT2-KMSA calculations of CO_2 solubility and vapor phase mole fraction for the ternary CO_2 – H_2O – NaCl mixture, and dashed lines are model calculations of CO_2 solubility and vapor phase mole fraction for the salt-free binary CO_2 – H_2O mixture.

Finally, the new model predicts CO_2 solubilities in the mixed electrolyte solutions and brines very accurately, without any additional adjustable parameter. An example is shown in Figure 21 for the solubility of CO_2 at three different temperatures in a synthetic brine of ionic strength equal to 1.712 mol/kg.

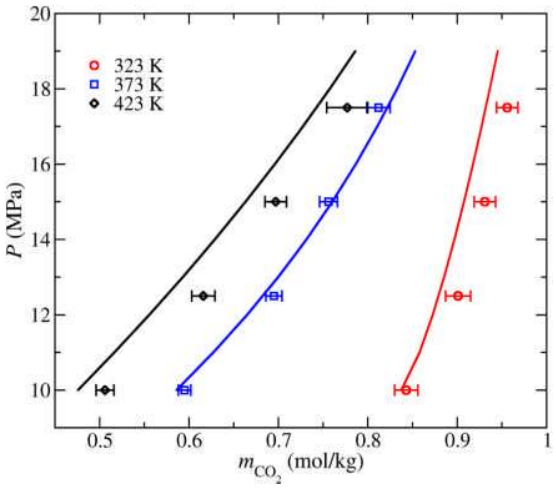

Figure 21. CO_2 solubilities in synthetic brine A (I = 1.712 mol/kg) at 323 K, 373 K and 423 K. Symbols are literature experimental data and lines are SAFT2-KMSA predictions.

In conclusion, the proposed SAFT2-KMSA model shows great predictive power for the study of CO_2 solubilities in mixed elecrolyte solutions and brines and can be used reliably for CCS process design.

More details on this work can be found at: H. Jiang, A.Z. Panagiotopoulos and I.G. Economou, "Modeling of CO_2 Solubility in Single and Mixed Electrolyte Solutions Using Statistical Associating Fluid Theory", *Geochimica et Cosmochimica Acta,* **176**, 185 – 197 (2016).

Numerical Modelling of Brittle Fracture Propagation in a Steel Pipeline Transporting CO_2

R.H. Talemi[1], S. Brown[2], S. Martynov[3], H. Mahgerefteh[3]

[1]*ArcelorMittal Global R&D Gent-OCAS N.V., Pres. J.F. Kennedylaan 3, 9060 Zelzate, Belgium*

[2]*Present address: Department of Chemical and Biological Engineering, University of Sheffield, S1 3JD, U.K.*

[3] *Department of Chemical Engineering, University College London, London WC1E 7JE, U.K.*

It is widely accepted that economically viable long-distance transportation of CO_2 in Carbon Capture and Sequestration projects can be achieved using pipelines transmitting dense-phase CO_2 fluid at pressures in excess of *ca.* 90-150 bar. Given that such pipelines are likely to pass close to residential areas their accidental failure may result in release of significant amount of CO_2 posing potential risks of asphyxiation by the toxic cloud. Of particular concern for CO_2 pipelines are long running fractures, damaging long pipeline sections and resulting with rapid releases of large amount of CO_2. In order to minimise the chances of CO_2 pipeline failure, the pipeline material, diameter and wall thickness, as well as measures minimising the consequences of the failure (e.g. placement of the pipeline crack arrestors) are carefully selected in the design, relying on predictions using mathematical models of fracture propagation and arrest. In the contrast to natural gas transportation pipes, which can be susceptible to ductile fractures, it has recently been suggested that unusually high Joule-Thomson coefficient of CO_2 escaping from an accidently damaged pipeline may lead to significant cooling and loss of ductility of the pipeline material, increasing the risks of brittle fracture propagation (Mahgerefteh & Atti, 2006; Cosham *et al*, 2015).

In the present study a coupled Fluid-Structure Interaction (FSI) model for simulating dynamic brittle fracture in buried pressurised CO_2 pipelines is developed and applied to evaluate the risk of brittle fracture propagation in a real-scale 1.22m diameter API X70 steel pipeline, transporting CO_2 at 0°C and 11 MPa.

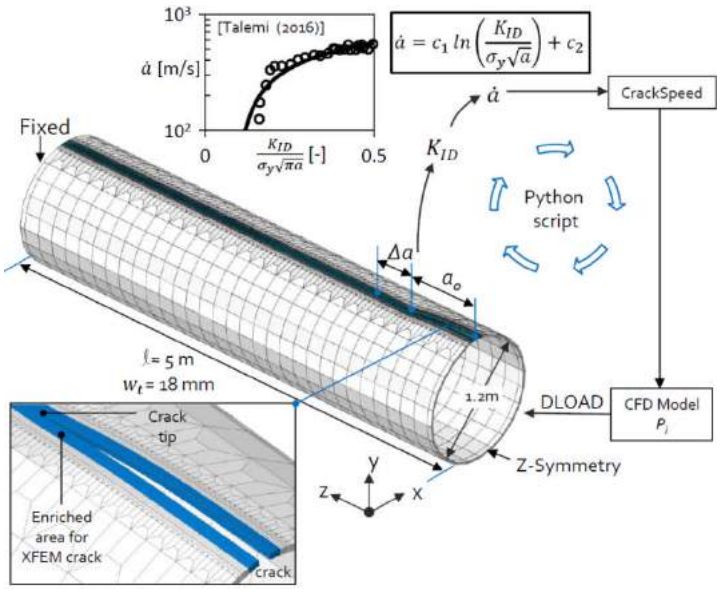

Figure 22. Three-dimensional finite element mesh discretisation of a simulated pipe section along with the schematic representation of the developed coupling algorithm for modelling running brittle fracture and pipeline decompression.

Coupled FSI Model

To simulate the state of the flow in the rupturing pipeline, a compressible one-dimensional Computational Fluid Dynamics (CFD) model is applied, where the pertinent fluid properties are determined using a thermodynamic model. In terms of the fracture model, an eXtended Finite Element Method (XFEM) is used to model the dynamic brittle fracture behaviour of the pipeline steel by assuming a stationary crack, for which the crack tip position can be correlated with the crack propagation velocity and the stress intensity factor K_{ID}.

Figure 22 illustrates the FSI algorithm for coupling the pipeline running brittle fracture model with the CFD code predicting the decompression of a pipe with a moving crack. At the start of the simulation the bulk fluid pressure, P, and the corresponding crack tip pressure, P_i, are calculated by the CFD model for an arbitrary small initial longitudinal crack opening along the major axis of the pipeline, formed for example, as a result of third-party damage. The pipeline internal and back-fill pressure loads are next setup in ABAQUS using the DLOAD subroutine to predict the state of deformation of the pipeline. Then, for an arbitrary small time increment, Δt, pipeline rupture is simulated in ABAQUS using XFEM method for a given internal and back-fill pressure loads setup at the pipe wall using DLOAD subroutine. A Python script was written to repeat the above procedure up to the point at which the crack tip position reaches the end of the pipe.

More information about the relation between the crack propagation speed and K_{ID} can be found in previous work (Telemi, 2016).

Results and Discussion

The developed coupled model allows the quantitative prediction of the pipeline prone to long running fractures in the form of the variation of crack length with crack propagation velocity. Figure 23 compares the crack propagation speeds predicted by the crack propagation model (XFEM) assuming constant pipeline pressure, the developed coupled FSI model (XFEM+CFD) and the CFD model coupled with analytical HLP equation for the crack propagation, for both upper and lower shelf CVN energies (HLP+CFD).

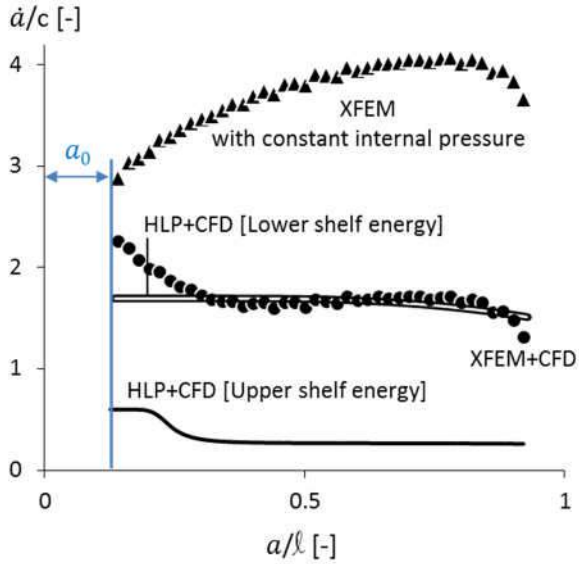

Figure 23. Normalized crack propagation velocity (c=343m/s) versus normalized crack propagation length.

From the results in Figure 23 it can be seen that the XFEM predictions for the constant internal pressure lead to overestimation of the crack propagation velocity and gradual increase in the crack speed with the crack length. The main reason for this behaviour is that the ratio between internal pressure and external pressure does not change as the crack propagates, because there is no decompression while brittle fracture is occurring. Comparing the results of

XFEM+CFD model with the HLP+CFD approach

Figure 24. Contour plot distribution of displacement in *X*-direction at different crack propagation time steps.

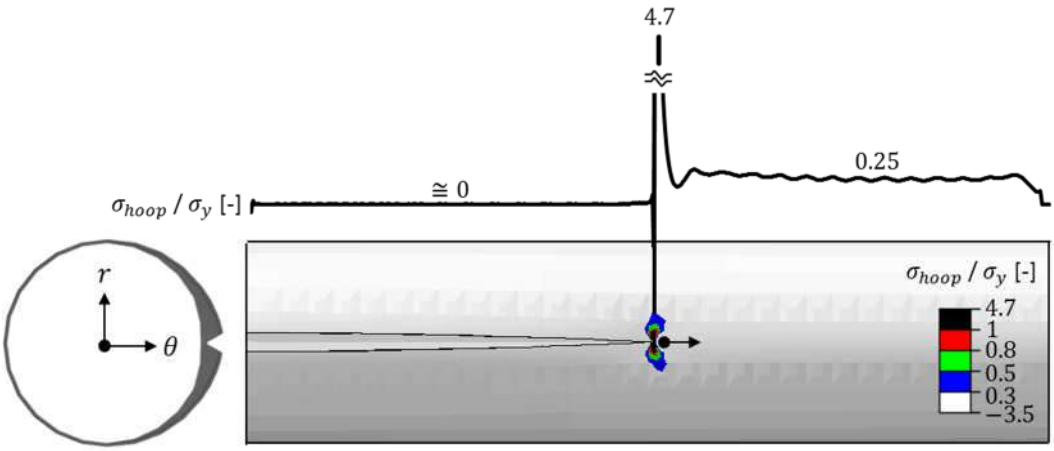

Figure 25. Instantaneous shape of the pipe with a running brittle crack, the stress distribution at crack tip and variation of the normalised hoop stress distribution in the axial direction.

at lower shelf energy proves that the crack propagation speed predicted using the coupled XFEM-CFD model is in a good agreement with the estimates based on the HLP equation.

Figures 24(a) and (b) show the deformed shape of the pipe at different time steps. The figures show contour plots of the pipe wall displacements in *X* direction, U_{xx}. It can be seen that at t = 7.53 ms the pipe is opening and the maximum displacement is around 381 mm.

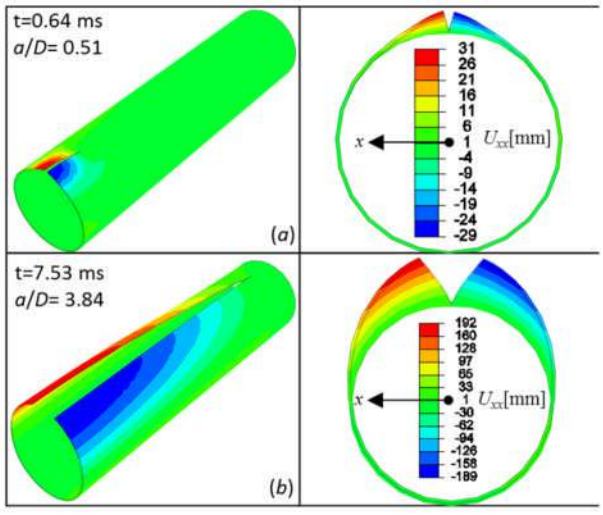

Figure 25 illustrates the running brittle crack in the pipe, the stress distribution at the crack tip and the normalised variation of hoop stress distribution inside the pipe along the crack propagation path. As it is shown in the figure the stress distribution of the pipe can be transformed to cylindrical coordinate system, which results in radial, hoop (circumferential or tangential) and axial (longitudinal) stresses. In case of the pipe model, the hoop stress is the acting stress to open the crack. As it can be seen from the figure, the hoop stress is almost zero at the fractured part of the pipe and reaches its maximum around 4.7 times of the yield stress, at the crack tip. The hoop stress decreases down to 0.25 times of yield stress in the pressurised side (i.e. un-fractured section) of the pipeline.

Figure 26 shows the comparison between crack propagation and CO_2 decompression velocities obtained for a pre-combustion CO_2 mixture containing 93.1% of CO_2, 3.5% of N_2 and 3.4% of H_2S.

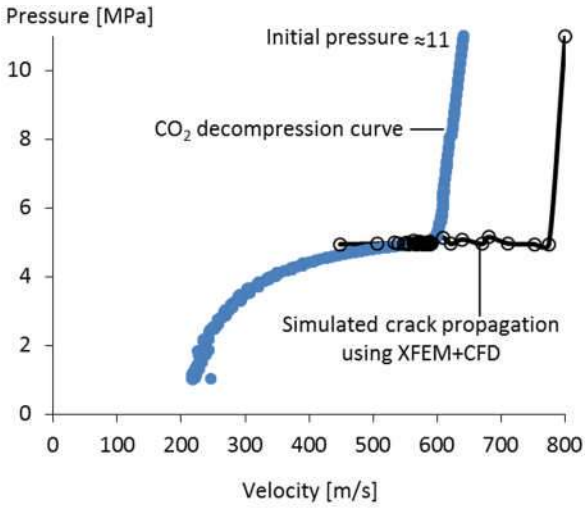

Figure 26. A comparison between the variation of gas pressure versus decompression velocity for CO_2 and the predicted crack velocity during decompression.

From the figure it can be concluded that around crack tip pressure of 4.5 MPa the predicted crack propagation velocity becomes lower than the gas decompression velocity curve, which indicate that, in case of having brittle fracture, the propagating brittle crack is being arrested.

Conclusion

In this study, a coupled FSI model has been introduced to simulate brittle fracture propagation in a CO_2 pipeline. Using the developed model it was possible to couple the fluid dynamics of the escaping fluid during decompression and the propagating brittle fracture of the deforming pipeline. From the obtained results it can be concluded that in case of having brittle fracture, the propagating crack is being arrested after some crack propagation steps and there is no risk of brittle fracture propagation in API X70 pipeline steel transporting CO_2 streams. The model developed will be useful to investigate the effects of CO_2 stream composition on the brittle fracture behaviour of steel pipelines transporting impure CO_2.

References

Mahgerefteh, H., & Atti, O. (2006). Modeling low-temperature-induced failure of pressurized pipelines. *AIChE Journal*, 52(3), 1248–1256.

Cosham, A., Koers, R., Andrews, R., & Schmidt, T. (2015). Progress towards the new eprg recommendation for crack arrest toughness for high strength line pipe steels. *In 20th JTM, 3-8 May 2015, Paris, France.*

Talemi, R.H., 2016. Numerical simulation of dynamic brittle fracture of pipeline steel subjected to DWTT using XFEM-based cohesive segment technique. *Fracture and Structural Integrity* 36, 151–159.

Efficient Thermodynamic Interpolation Scheme for the Simulation of Two-Phase Flow of CO_2 Mixtures

I. Economou[1], L. Peristeras[1], D. Tsangaris[1], S. Brown[2], S. Martynov[3]

[1]*National Center for Scientific Research "Demokritos", Athens, Greece*

[2]*Present address: Department of Chemical and Biological Engineering, University of Sheffield, S1 3JD, UK*

[3] *Department of Chemical Engineering, University College London, London WC1E 7JE, U.K.*

Solving the CFD models describing flows of CO_2 and its mixtures relevant to the various stages of Carbon Capture and Storage (CCS) scheme, requires fluid property values (e.g. pressure, temperature, speed of sound, phase fractions) as continuous and smooth functions of two state variables. In thermodynamic modeling a variety of schemes is available using the so-called equations of states (EoS). The computational time needed for executing these schemes varies and, in general, increases with the complexity of the EoS (Brown et al, 2015). By today's standard if the EoS selected has the complexity of EoS based on Statistical Associating Fluid Theory (SAFT) it is practically difficult to incorporate it directly into a CFD software. In addition to the computational burden, the use of advanced Equations of State in CFD simulations becomes problematic when physical properties are evaluated near the phase transitions states or at the critical region. These problems are not seen with cubic EoS because the later EoS have a smooth behavior (including extrapolation) and their roots needed for density calculation are calculated analytically.

In order to address the above problems within the scope of CO_2 mixtures CFD/flow simulations, a new methodology has been developed by the partners from NCSR "Demokritos", and University College London (UCL), which enables calculation of two-phase envelopes in a robust and efficient manner, and uses interpolation method for efficient "on-the-fly" calculation of the thermodynamic properties in the CFD simulations.

PC-SAFT Equation of State

In the present study in order to predict the properties of CO_2 and its mixtures, the Perturbed Chain-Statistical Associating Fluid Theory (PC-SAFT) EoS presented by Diamantonis *et al.* (2013) is applied and therefore, a brief description is provided. The PC-SAFT EoS is expressed as the summation of residual Helmholtz free energy terms that occur due to different types of intermolecular interactions between the various components in the system under study. The residual Helmholtz free energy, A_{res} is equal to the Helmholtz free energy minus the Helmholtz free energy of the ideal gas at given temperature and density. For a system that consists of associating chains (for example aqueous mixtures), PC-SAFT can be expressed as (Diamantonis et al., 2013):

$$\frac{A^{res}(\rho,T)}{NRT} = \frac{a^{hs}}{RT} + \frac{a^{chain}}{RT} + \frac{a^{disp}}{RT} + \frac{a^{assoc}}{RT},$$

where a is the Helmholtz free energy per mole, R is the universal gas constant and the superscripts "res", "hs", "chain", "disp", and "assoc" refer to residual, hard sphere, chain (hard chain reference fluid), dispersion, and association, respectively.

Rapid Interpolation Method

As described previously, the coupling of an EoS with the CFD model describing two-phase flow is complicated by the fact that the free variables are the density, ρ, and internal energy, e, based on which the system pressure, P, and temperature, T, must be determined using iterative procedure when using an EoS (in this case PC-SAFT) which is explicit in ρ and T. To overcome this issue we introduce two interpolant grids, one of which is constructed using the P and T as free variables, and the other using ρ and e. In the P-T space the

grid points are sampled along isotherms which are uniformly distributed within the temperature range and use higher concentration of points along the isotherms near to the bubble point and dew point phase transition lines. These grids then provide the means for rapidly computing the thermodynamic properties and phase equilibria in the CO_2 flow simulations (Brown et al, 2016).

Results

The newly introduced methodology for rapid interpolation of the thermodynamic properties data was developed using PC-SAFT for binary and quinternary CO_2 mixtures. Figure 27 show the {ρ, e} interpolation grids constructed for a binary mixture using both uniform and non-uniform {P, T} grids. As can clearly be seen in Figure 27 (top panel) the "uniform" sampling strategy produces a much sparser weighting of the points through the phase envelope compared to the one achieved in Figure 27 where the re-distribution of the points results in a much greater number of samples between the dew and bubble point lines. The latter enables better resolution of the properties near the phase transition regions, which is important to guarantee accurate results of calculations of two-phase CO_2 flows.

The developed interpolation method has been implemented in a CFD code developed by UCL to predict the physical properties of CO_2 rich mixtures in the pipeline rupture simulations using a two-phase flow model based on the homogeneous equilibrium mixture assumption.

In particular, full-bore rupture scenarios of CO_2 pipeline decompression have been simulated for comparison with the real test data.

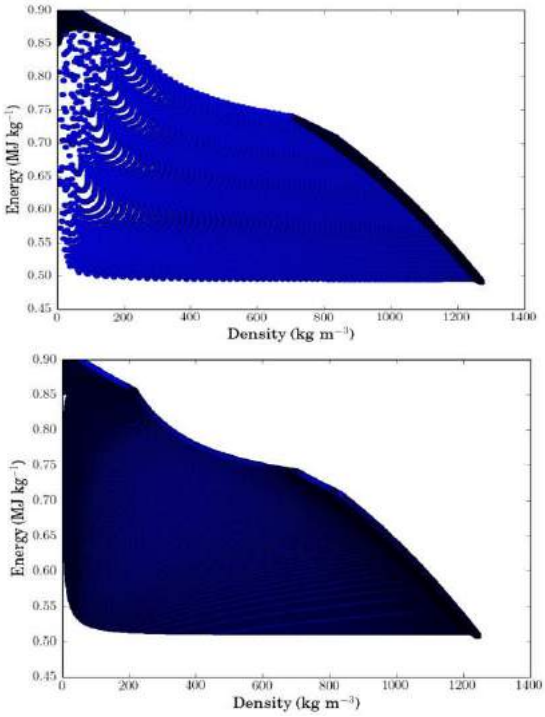

Figure 27. The {ρ, e} interpolation grids in the case of a uniform sampling (top) and with the adaptive sampling method (bottom) produced for the binary mixture of 95.96 %CO_2 - 4.04 % N_2 (vol/vol).

Figure 28 shows an example of the thermodynamic trajectory at the closed end of the pipeline section during its full-bore rupture, relative to the dew and bubble lines. As may be observed, during the initial decompression the fluid drops almost instantaneously along the isentropic line into the phase envelope where it descends towards the dew line at low temperatures.

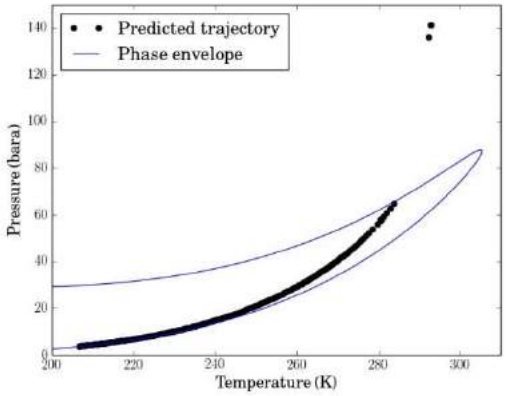

Figure 28. Thermodynamic trajectory of the decompression relative to the binary mixture phase envelope at the closed end of the pipeline following the initiation of decompression.

The results of simulations using the above interpolation scheme implemented into a pipeline decompression model showed that the CFD model predictions are in good agreement with the experimental data, while the interpolation approach enables a flexible and robust mechanism to obtain thermodynamic properties data.

References

Diamantonis, N.I., Boulougouris, G.C., Tsangaris, D.M., Kadi, M.J. El, Saadawi, H., Negahban, S., Economou, I.G., 2013b. Thermodynamic and transport property models for carbon capture and sequestration (CCS) processes with emphasis on CO_2 transport. *Chem. Eng. Res. Des.* 91, 1793–1806.

S. Brown, S. Martynov, H. Mahgerefteh, D.M. Tsangaris, G.C. Boulougouris, I.G. Economou and N.I. Diamantonis, “Impact of Equation of State on Simulating CO_2 Pipeline Decompression”, *Proc. Safety Envir. Prot.,* submitted, November 2015.

S. Brown, L.D. Peristeras, S. Martynov, R.T.J. Porter, H. Mahgerefteh, I.K. Nikolaidis, G.C. Boulougouris, D.M. Tsangaris and I.G. Economou, “Thermodynamic Interpolation for the Simulation of Two-Phase Flow of Complex Mixtures”, *Computers & Chem. Eng.,* to be submitted, May 2016.

Modeling of Impurities Effects on Processes in CO_2 Geological Storage

A. Niemi[1], F. Fagerlund[1], M. Hedayati[1], R. Herbert[1], F. Basirat[1], B. Jong[1], M. Rasmusson[1] and A. Wigston[2]

[1]*Uppsala University, Sweden*
[2]*Canmet ENERGY, Canada*

During the period, Uppsala University, Sweden in collaboration with CanMet, Canada has investigated several issues relevant to geological storage of CO_2 in the presence of impurity gases in the injected gas mixture. The main topics addressed include (i) geochemical effects of impurities to the mineral and brine composition, (ii) effect of impurities to CO_2 dissolution into brine, in particular to the convective mixing process that is believed to enhance dissolution and (iii) effect of impurities to the movement of the CO_2 rich gas-mixture. Some of the findings are exemplified below.

Experiment-based batch chemical modeling

CanmetENERGY-Ottawa, Canada has carried out batch experiments with reservoir and cap-rock samples from the main field investigation site of the project the, the Heletz site in Israel. These experiments have addressed the changes in mineral and fluid composition when the samples are in contact with pure CO_2 or CO_2 containing impurity gases. The overall objectives is to understand the interaction between pure and impure CO2 with minerals under 60°C temperature and 145 bar pressure (in-situ conditions). At Uppsala, the modeling of the experiments was carried out using TOUGHREACT V3.0-OMP model (Xu et al., 2014). The geochemical model is calibrated by adjusting reactive surface area as controlling parameter for kinetic rate calculation of minerals to find the best match with experimental data. The objectives are to understand the precipitation and dissolution of minerals in such a system, to estimate the mineral composition heterogeneity within the reservoir core sample and to determine kinetic rate of minerals that could be used to predict the coupled processes of fluid flow and geochemical reactions during Heletz site field scale experiment.

Based on evaluation of ion concentrations and mineral composition at the experimental results, the dissolution and precipitation rate of minerals are estimated. The predicted results by model revealed that some minerals are far from equilibrium condition at the end of experiment duration of impure SO_2 (36 day). Ankerite dissolves partially and consequently Fe+2 and Ca+2 concentration increases in the system. Pyrite precipitates with a higher rate than Anhydrite, so that after 36 days, Pyrite is detected in the XRD results while Anhydrite volume is too small to be identified. Model predicts that after one year 3.4% Anhydrite precipitates while Ankerite completely dissolves and the system reached a steady-state equilibrium condition. A longer experimental period is required in order to validate model predictions. Figure 29 shows a preliminary model prediction and experimental results for impure CO_2 test under duration of the experiment.

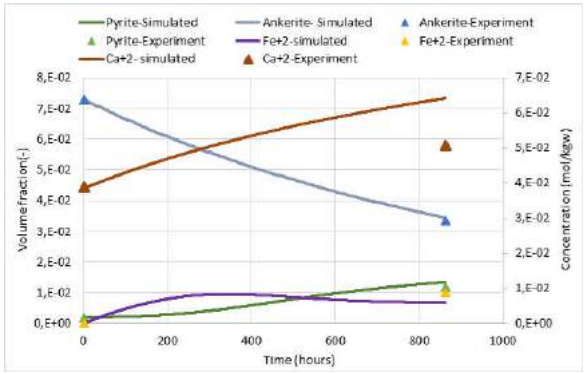

Figure 29. Preliminary result on the evolution of some key minerals in the presence of SO_2 impurity gas.

Effects of co-injected impurities on the enhanced solubility trapping of CO_2 during geological storage

Solubility trapping is one of the most important mechanisms to ensure secure geological storage of CO_2 over large time scale. As CO_2 dissolves into formation brine density changes are induced, triggering convective mixing that greatly enhances the solubility trapping rate. However, the potential impacts of co-injected impurities on this enhanced solubility trapping remain to be determined. We investigate the effects of several co-contaminants (N_2, CH_4 and H_2S) on the enhanced solubility trapping.

The study was conducted by using SUTRA-MS (Hughes and Sanford, 2004) for multi-component density-driven flow simulations, as well as, by using a newly developed in-house analysis tool (Figure 30), accounting for the impurity effects on both solubility and the induced density changes driving the convective mixing. We show that co-injection of N_2, CH_4 and H_2S during CO_2 storage have negative effects on convective mixing. Co-injection increases the time scale and decreases the rate of CO_2 solubility trapping (Figures 31 and 32). Of the investigated co-contaminants, H_2S due to its relatively high solubility had the largest effect on the CO_2 solubility trapping even at small concentrations.

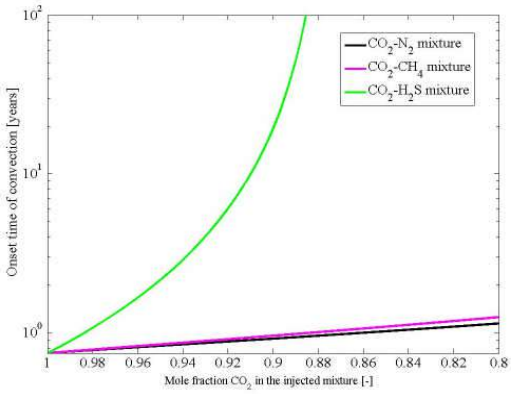

Figure 31. The onset time of convection for various gas-mixtures.

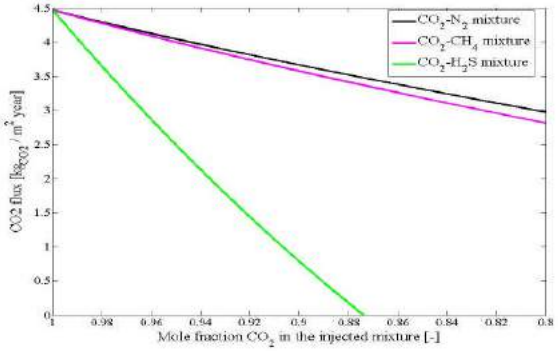

Figure 32. The steady convective flux of CO_2 for various gas-mixtures.

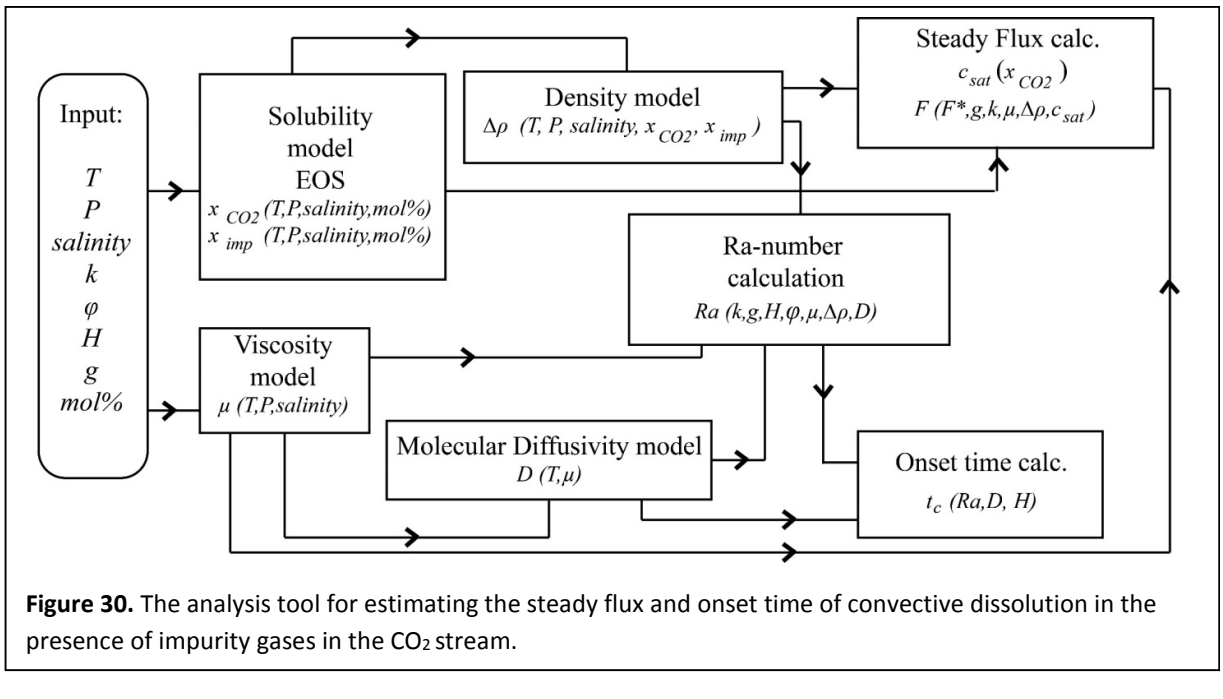

Figure 30. The analysis tool for estimating the steady flux and onset time of convective dissolution in the presence of impurity gases in the CO_2 stream.

Effect of impurities to the movement of the CO2 rich free phase

We have also investigated the effect of impurities on the actual movement and spreading of the CO_2 rich gas/supercritical phase. For this work, the numerical code TOUGH2 (Pruess, 1999) along with the equation of state module ECO2N was modified to take into account the properties of the gas mixtures. For each time step, the relevant flow properties of the CO_2 rich (gas/supercritical) phase are calculated as those for the gas mixture, then each component is allowed to dissolve according to its specific rate, after which the composition of the CO_2 rich phase is updated for the next step. Four common impurities, i.e. N_2, SO_2, H_2S and CH_4 were considered and as an example of an industrial scale project case similar to the Sleipner site was selected. An example of simulated gas distribution is shown in Figure 33 for the case of pure CO_2 and CO_2 mixture with 10% of N_2, the gas mixture that had the biggest effect.

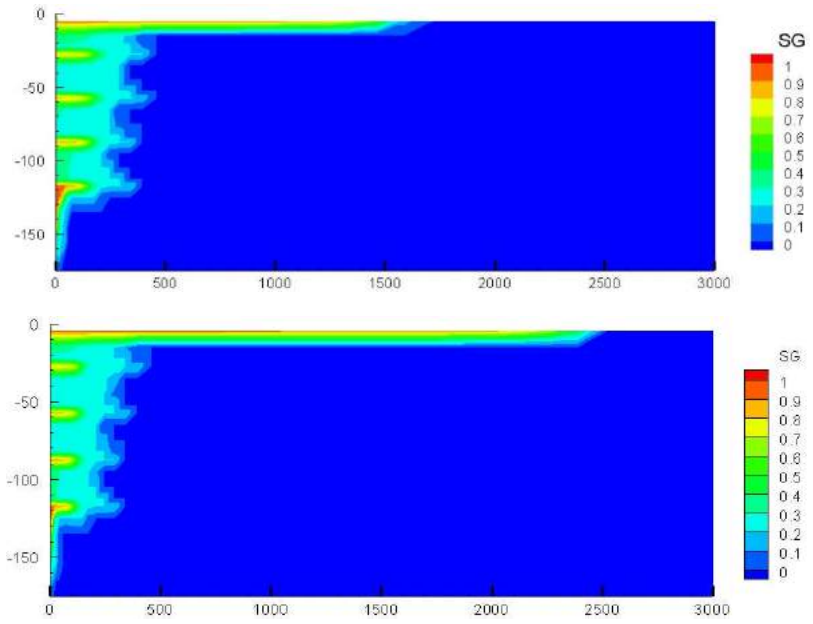

Figure 33. Example of simulated gas/supercritical phase spreading in the reservoir layers after 20 years form the start of injection; pure CO_2 (upper panel) and CO2 with 10% N_2 (lower panel).

The 2nd CCS Forum

A.M.E. Ward and M. Fairweather

University of Leeds, UK

CO2QUEST held its third and final Technical Meeting at the St. George Lycabettus hotel in Athens, Greece, on Wednesday 16th and Thursday 17th December 2015.

The **2nd International Forum on Recent Developments of CCS Implementation** was co-organised with CO_2QUEST's sister project IMPACTS. Both consortia are concerned with the effect of impurities on the transport of CO_2 mixtures from power stations and other CO_2-intensive industries. The projects use newly developed state-of-the-art mathematical models and large-scale experiments to make recommendations for the safe design and economic operation of CCS.

Figure 34. Prof. Haroun Mahgerefteh introducing the CO_2QUEST project.

Both programmes were approaching near-completion at the time of the event. As such, it provided an invaluable opportunity for the partners to conclude the current state-of-play in this field, and to summarise the research advances that have been made over the last few years. It was apparent that there was complementary work to be disseminated between the projects, and that collaboration could be a possibility for future H2020 calls.

The agenda was not limited to this topic, and foremost representatives from academia, industry and governance were welcomed to submit contributions on all aspects of the CCS value-chain. Over 35 oral presentations (including 4 keynotes) were delivered across four technical sessions: Transport and Safety, Process Optimisation and Techno-economic Considerations, Thermophysical Properties and Storage. Additionally, a poster session was held during the breaks to promote ongoing discussion and networking.

The aim of the event was to provide an update on the current status of CCS implementation within the EU and internationally. Just weeks before the workshop, the UK government announced that it was cancelling the £1bn CCS technology competition, creating levels of uncertainty within the UK. However, there have been some positive developments overseas and Dr Greeshma Gadikota, an invited speaker from Columbia University provided an overview of CCS developments within the US, spanning fundamental research to implemented technologies including large-scale demonstration facilities. It is obvious that there is still a lot to do to make CCS a commercially viable technology, especially within the EU, but it is events like the CCS forum that help to promote this message and expand the research community.

Figure 35. Dr Greeshma Gadikota giving her talk titled 'CCS Developments in North America'.

The event attracted a diverse audience, with 65 delegates from over 20 different institutions in attendance. We would like to thank everyone that participated in not just this event, but the three workshops that have been held since CO2QUEST started.

Figure 36. Delegates from 13 different countries were in attendance at the 2nd CCS Forum.

Special thanks goes to Dr. Marit Mazzetti and An Hilmo, SINTEF, for their significant contributions in organising the workshop, and to Katie Welch at Imperial College London for helping to ensure that it ran smoothly.

A special issue of the International Journal of Greenhouse Gas Control has been associated with this event. The SI is due to publish late 2016/early 2017 and 15 full papers on the topic of impurities have currently been submitted for review by our guest editors.

Event material including a book of summaries and copies of the presentations can be downloaded from the project website: http://www.co2quest.eu/ccsforum15.htm

Congratulations to CO2QUEST's…

Reza Hojjati, ArcelorMittal Global R&D Gent (OCAS)

During the Simulia Benelux regional users meeting in October 2015, Reza was awarded the Laureate Presentation Award for his presentation "Numerical modelling of dynamic brittle fracture using XFEM-based cohesive zone approach".

Prof. Zhang, Dalian University of Technology (DUT)

In April 2015, Prof. Zhang received a Gold Award at the 43rd International Exhibition of Inventions in Geneva for the invention "Distillation Technology by Cryogenic Adsorption" for CO2 capture and purification applications.

Publications

For regular updates on publications please visit:
http://www.co2quest.eu/publications.htm

Events

Material from CO_2QUEST organised events can be found here: http://www.co2quest.eu/events.htm

Acknowledgement and Disclaimer

The authors gratefully acknowledge funding received from the European Union's Seventh Framework Programme for research, technological development and demonstration under grant agreement number 309102.